

Spectral, polarisation and time-lag properties of GRS 1915+105 radio oscillations

R. P. Fender¹ D. Rayner², S. A. Trushkin³, K. O'Brien¹, R. J. Sault²,
G. G. Pooley⁴, R.P. Norris²

¹ Astronomical Institute ‘Anton Pannekoek’, University of Amsterdam, and Center for High Energy Astrophysics, Kruislaan 403, 1098 SJ, Amsterdam, The Netherlands rpf@astro.uva.nl

² Australia Telescope National Facility, CSIRO, PO Box 76, Epping NSW 2121, Australia

³ Special Astrophysical Observatory, RAS, Nizhnij Arkhyz, Karachaevo-Cherkassia 369167, Russia

⁴ Mullard Radio Astronomy Observatory, Cavendish Laboratory, Madingley Road, Cambridge CB3 OHE ggp1@cam.ac.uk

24 October 2018

ABSTRACT

We report high sensitivity dual-frequency observations of radio oscillations from GRS 1915+105 following the decay of a major flare event in 2000 July. The oscillations are clearly observed at both frequencies, and the time-resolved spectral index traces the events between optically thin and thick states. While previously anticipated from sparse observations and simple theory, this is the first time a quasi-periodic signal has been seen in the radio spectrum, and is a clear demonstration that flat radio spectra can arise from the combination of emission from optically thick and thin regions. In addition, we measure the linear polarisation of the oscillations, at both frequencies, at a level of about 1–2%, with a flat spectrum. Cross-correlating the two light curves we find a mean delay, in the sense that the emission at 8640 MHz leads that at 4800 MHz, of around 600 seconds. Comparison with frequency-dependent time delays reported in the literature reveals that this delay is variable between epochs. We briefly discuss possible origins for a varying time delay, and suggest possible consequences.

Key words:

binaries: close – stars: individual: GRS 1915+105 – infrared: stars – radio continuum: stars – ISM:jets and outflows

1 INTRODUCTION

GRS 1915+105 is a luminous and spectacularly variable source of radiation from radio through to hard X-ray regimes. Its behaviour in both hard and soft X-rays is unique (e.g. Foster et al. 1996; Morgan, Remillard & Greiner 1997; Belloni et al. 2000), and it is a celebrated source of relativistic jets (Mirabel & Rodríguez 1994; Fender et al. 1999; Rodríguez & Mirabel 1999; Dhawan, Mirabel & Rodríguez 2000; Giovannini et al. 2001).

X-ray flux variations on a variety of timescales have been interpreted as the repeated draining and refilling of the inner accretion disc, possibly due to extremely rapid transitions between ‘canonical’ black hole accretion states (e.g. Belloni et al. 1997a,b; Feroci et al. 1999; Belloni et al. 2000); however the physical meaning of these apparent changes in inner disc radius is not entirely certain (Merloni, Fabian & Ross 2000). Quasi-sinusoidal oscillations with similar periods, almost certainly the signature of synchrotron emission

from repeated ejection events, have been observed at radio, millimetre and infrared wavelengths (Pooley & Fender 1997; Fender et al. 1997; Eikenberry et al. 1998, 2000; Mirabel et al. 1998; Fender & Pooley 1998, 2000). These oscillations appear to have a direct connection to the X-ray dips (Pooley & Fender 1997; Eikenberry et al. 1998, Mirabel et al. 1998, Klein-Wolt et al. 2001), although there is some debate as to whether they are associated with ‘soft’ (e.g. Naik & Rao 2000) or ‘hard’ (e.g. Klein-Wolt et al. 2001) X-ray states. Delays between different radio bands (Pooley & Fender 1997; Mirabel et al. 1998) and between the infrared and radio bands (Mirabel et al. 1998; Fender & Pooley 1998) clearly indicate that optical depth effects play an important role in the observed emission from these ejections. Details such as the magnitude and variability of these delays are crucial for gaining a quantitative understanding of the outflow process.

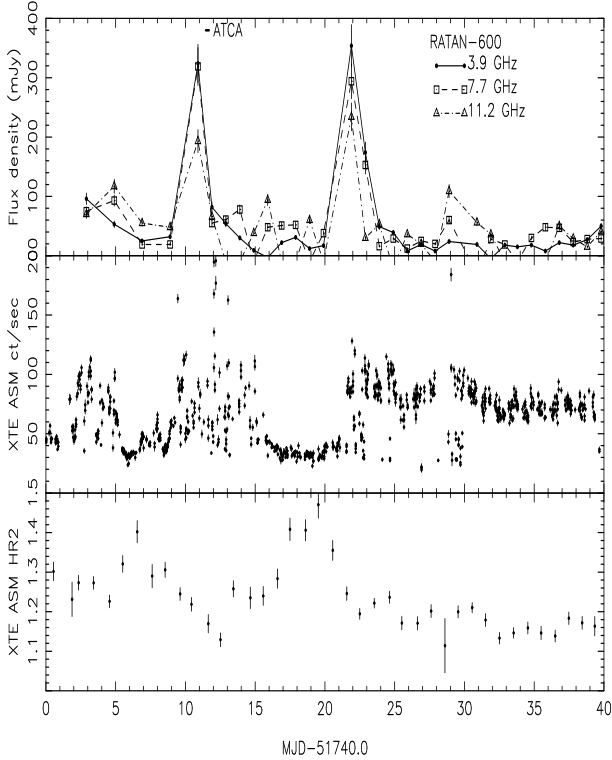


Figure 1. Radio and X-ray monitoring of GRS 1915+105 before and after the ATCA observations (which are indicated by a bar in the top panel). Note that the XTE ASM total count rate is based upon individual scans, whereas the HR2 colour is based on daily averages. The RATAN radio data reveal two major flaring episodes. The first, during the decay of which our ATCA observations were made, may be associated with the brief hard X-ray state around MJD 51746, or may be associated with the subsequent week-long ‘plateau’ between MJD 51755–62.

2 OBSERVATIONS

2.1 RATAN-600

The RATAN-600 observations were carried out as a part of a monitoring program of microquasars to study their flare activity across a broad frequency range. Observations were performed at 3.9, 7.7, 11.2 and 21.7 GHz; the 3–11 GHz data are presented in the top panel of Fig 1. The flux density calibration was performed using observations of 3C286 (1328+30) and PKS1345+12. Although interference sometimes prevented realisation of the maximum sensitivity of the radiometers, daily observations of reference sources indicate that the error in the flux density measurements for 1915+10 did not exceed 5–10% at 2.3, 3.9, and 11.2 GHz and 10–15% at 21.7 GHz. For further details see Trushkin, Majorova & Bursov (2001).

2.2 XTE ASM

We have made use of public data from the Rossi X-ray Timing Experiment (XTE) All-Sky Monitor (ASM; Levine et al. 1996). These data are available at xte.mit.edu. The total intensity and HR2 X-ray colour (ratio of counts in 5–12 to 3–5 keV bands) are presented in Fig 1.

2.3 ATCA

We have observed GRS 1915+105 with the Australia Telescope Compact Array (ATCA) for approximately six hours on 2000 July 26. The override observations were triggered as a result of the radio flare observed by the RATAN-600 telescope around MJD 51750. At this time the array was in a compact configuration. As a result, in order to reduce the effects of field sources (see e.g. Chaty et al. 2001 for radio images of the field) we only used interferometer baselines $\geq 2200\text{m}$ at 4800 MHz. The compact configuration and relatively poor hour-angle coverage precluded any attempt to confidently calibrate Stokes V, and so we were not able to make a circular polarisation measurement.

In Fig 2 we present dual-frequency total intensity, spectral index and linear polarisation measurements of GRS 1915+105 obtained during the ATCA run. Care has been taken to check the reality of the low-level linear polarisation (ie. Stokes Q, U) measurements, and we are confident that those presented in Fig 2 are realistic. Mapping the data in linear polarisation produces results consistent with averaging the data presented in Fig 2. Note however that for the last few scans the polarisation calibration solutions were not good and those data are not used.

3 RESULTS

The 40-day light curves presented in Fig 1 clearly reveal the existence of radio flaring and dramatically varying X-ray flux and hardness. It has been previously established (e.g. Foster et al. 1996, Fender et al. 1999) that the prolonged (ie. more than a few days) hard states, or ‘plateaux’, are accompanied by flat or inverted spectrum radio emission and appear to be always followed by an optically thin radio flare. The inverted-spectrum emission probably corresponds to a powerful self-absorbed quasi-continuous jet (Dhawan et al. 2000; Fender 2001) and the optically thin post-plateau flares have been directly resolved into relativistically outflowing components (e.g. Mirabel & Rodriguez 1994; Fender et al. 1999). In terms of Fig 1, we consider the plateau phase to be between MJD 51756–51762, and its resultant flare to be the radio event which peaked around MJD 51762. What is less clear is whether the flare of \sim MJD 51750.0 was related to this subsequent plateau or to the shorter X-ray hard state around MJD 51746–51747. It is the decay of this flare, and the subsequent emergence of core-oscillation events, which were studied in detail with our ATCA observations. Note that there appears to be a third smaller flare associated with a drop in the X-ray flux around MJD 51768.

3.1 Optically thin decay

The characteristic decay and optically thin spectral index during the first two scans with ATCA (MJD 51751.45–51751.50) are indicative of ejecta from the observed outburst fading away as they propagate through the ISM, as directly imaged for previous outbursts by e.g. Mirabel & Rodriguez (1994), Fender et al. (1999). At a bulk velocity of $\geq 0.9c$ these synchrotron emitting clouds are likely to be by this stage hundreds of AU from the system and totally decoupled from the accretion process.

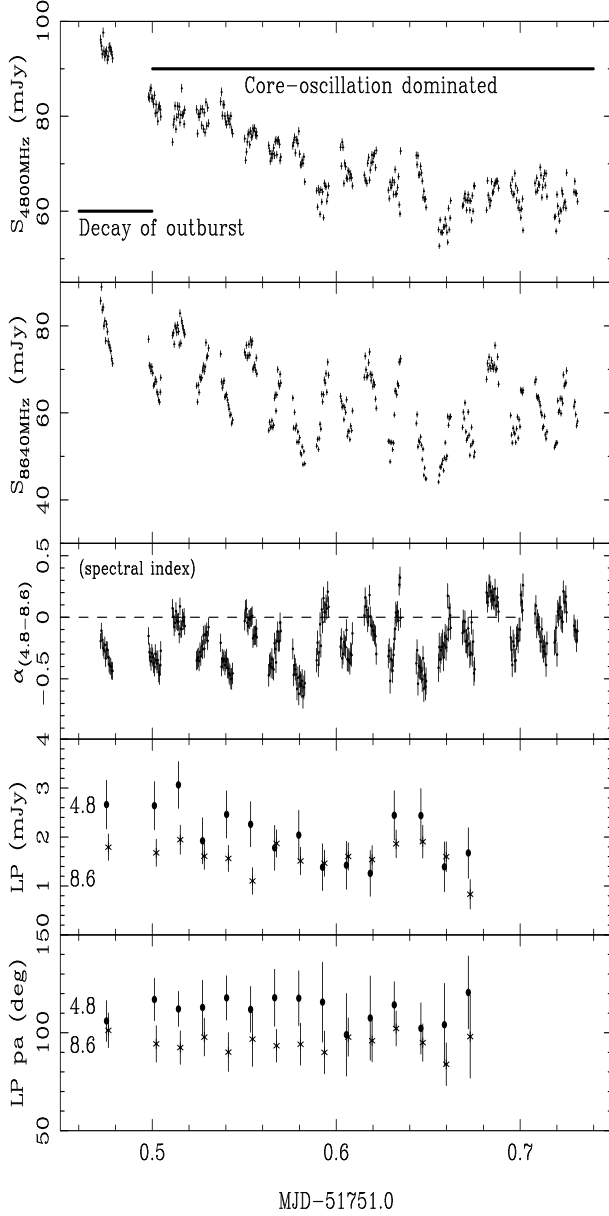


Figure 2. Dual-frequency observations of the transition from outburst to oscillating states in the radio emission from GRS 1915+105, following the first major flare indicated in Fig 1. The top three panels present 30-sec averaged data, the lower two panels 10-min averaged data. The spectral index, in the middle panel, is defined as $\alpha = \Delta \log S_\nu / \Delta \log \nu$. After \sim MJD 51751.55 the radio variability is dominated by oscillations, with a very clear signature in the spectral index. Linear polarisation, at the level of a few %, is clearly detected throughout the observation; note however that the polarisation calibration solutions became erratic for the last few scans and so those data are not presented here.

During these period the mean total intensities observed from GRS 1915+105 were ~ 90 mJy (4.8 GHz), and ~ 70 mJy (8.64 GHz), corresponding to a spectral index $\alpha = \Delta \log S_\nu / \Delta \log \nu \sim -0.4$.

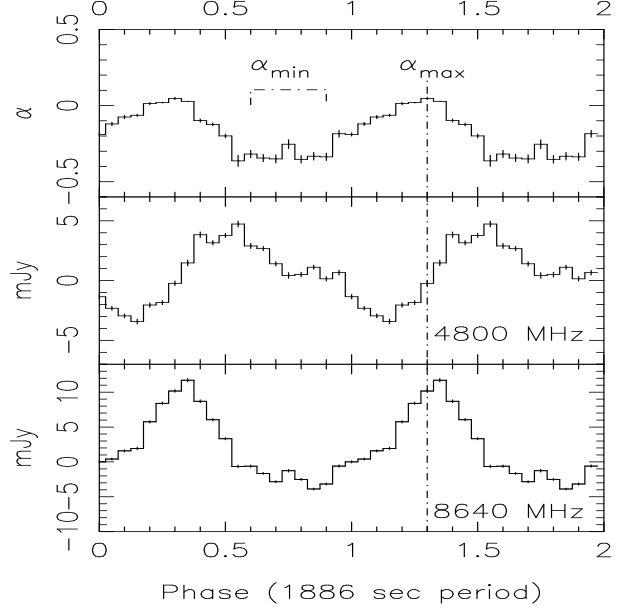


Figure 3. Spectral index, total flux density at 4800 and 8640 MHz, folded on a best-fit period for the oscillations of $0.02144d = 30.87$ minutes, in 20 equally-sized phase bins. Data from the first two scans (ie. prior to MJD 51751.5) have been excluded as they were dominated by the outburst decay.

3.2 Core oscillation events

After MJD 51751.51, the light curve and spectral index indicate a transition to radio oscillation events (Pooley & Fender 1997; Fender & Pooley 1998, 2000) which are known to be associated with rapid changes in the accretion flow (as indicated by simultaneous radio and X-ray observations – Pooley & Fender 1997; Mirabel et al. 1998; Klein-Wolt et al. 2001).

After this point the spectral index as plotted in Fig 2 clearly shows oscillations between optically thin ($\alpha_{\min} \sim -0.7$) and thick ($\alpha_{\max} \sim +0.2$). While it could be qualitatively appreciated from previous dual-frequency radio observations (e.g. Pooley & Fender 1997; Mirabel et al. 1998), this is by far the clearest illustration to date of the rapid changes in the spectral index of the emission from GRS 1915+105 during the radio oscillation events.

3.3 Polarisation and rotation measure

Linear polarisation was measured at both frequencies from GRS 1915+105 during both the optically thin and core-oscillation phases of our observations.

During the optically thin phase the mean linearly polarised flux densities were ~ 3 mJy (4.8 GHz) and ~ 1 mJy (8.64 GHz), corresponding to fractional linear polarisations were $\sim 3\%$ (4.8 GHz) and $\sim 2\%$ (8.6 GHz). During the transition to the oscillation phase the polarised flux density at 4.8 GHz drops significantly and becomes comparable to that at 8.6 GHz as the total intensity spectrum similarly flattens. The flattening of the linear polarisation spectrum, as well as the apparent halt in its initial decay at 4800 MHz, strongly suggest that it is associated with the core events and not remnant emission from the major optically thin ejection. Therefore we conclude that our data measure around 1 mJy of linearly polarised flux density associated with the oscilla-

tions at each frequency, corresponding to a fractional linear polarisation of 1–2%.

The position angles of the linear polarisation are similar for both phases, with averages for the entire run of $\text{pa}(4800 \text{ MHz}) = (112 \pm 2)^\circ$ and $\text{pa}(8640 \text{ MHz}) = (96 \pm 2)^\circ$. The 4800 MHz position angle is similar to that measured by MERLIN for the inner regions of the jet in Fender et al. (1999). Ascribing the difference in position angles to Faraday rotation, we can estimate a minimum rotation measure of $\sim 100 \text{ rad m}^{-2}$, with an associated intrinsic position angle of $\sim 90^\circ$ (neither exactly parallel or perpendicular to the observed jet axis). This is consistent with rotation measures of radio pulsars at distances of several kpc or more (e.g. Han, Manchester & Qiao 1999). However, this rotation measure seems to contradict the observations of Rodríguez et al. (1995) whose measurements of linear polarisation at three frequencies seem to imply an upper limit to the rotation measure of $\sim 50 \text{ rad m}^{-2}$. Possibly the magnetic field structure in the jet rotates between the regions from which the 8640 and (downstream) 4800 MHz emission arise. Whatever the intrinsic polarisation angle, the fact that the observed position angles remain approximately constant indicates the persistence over the observation of some magnetic field structure.

3.4 ‘Pulse folding’ the data

In order to understand the oscillations better, we have attempted to fold the data onto a single period. Using the Starlink package PERIOD, we have determined a best-fit single period of 0.02144 days, and folded the data onto that period. The detrended (see below) folded spectral index and total intensity light curves are plotted in Fig 3. The technique worked surprisingly well – there is a clear modulation in the folded light curves at both frequencies and in the spectral index, α . In fact the same period in the signal, to within 2%, was found in independent period searches on the 4800 and 8640 MHz data. It is clear that variations in α are dominated by the 8640 MHz light curve, which has significantly larger degree of modulation and as a result a clearer profile. From Fig 3 we can see that the lag between the two light curves is about 0.25–0.35 in phase, corresponding to 7–11 minutes, consistent with the lag obtained in the cross-correlation analysis below. We have also attempted to fold the polarised flux and position angle on the oscillation period. There is a hint in the folded light curves that the linearly polarised flux is modulating, but it is not statistically significant.

4 OPTICAL DEPTH TIME DELAYS

We have performed a cross-correlation analysis of the two lightcurves shown in Figure 2, using the discrete correlation function (DCF) of Edelson & Krolik (1988). Unlike the Interpolated Correlation Function (ICF) of Gaskell & Peterson (1987), which interpolates between individual points of the driving lightcurve (the lightcurve at 8640 MHz), the DCF determines the correlation coefficient at discrete time lags, which are then binned to create a uniformly sampled cross-correlation function. The DCF was preferred due to the large, quasi-regular gaps in the data and its ability to at-

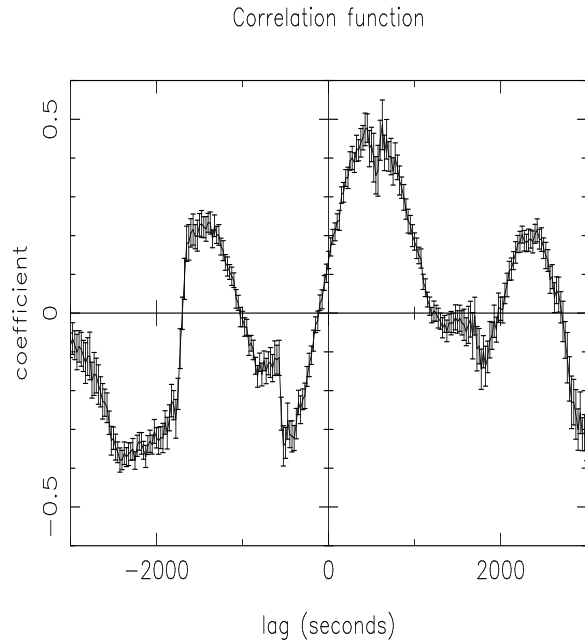


Figure 4. The discrete correlation function for the lightcurves at 8640 and 4800 MHz. A positive lag is defined to occur when variations in the 8640 MHz lightcurve precede those in the 4800MHz lightcurve.

Table 1. Summary of frequency-dependent time delays in GRS 1915+105

| MJD | ν_1 (Hz) | ν_2 (Hz) | Δt (sec) | |
|-------|----------------------|----------------------|------------------------|------|
| 50227 | 15×10^9 | 8.3×10^9 | ~ 250 | PF97 |
| 50583 | 15×10^9 | 8.3×10^9 | ~ 750 | M98 |
| | 8.3×10^9 | 5×10^9 | ~ 940 | M98 |
| 50700 | 1.4×10^{14} | 8.3×10^9 | ~ 860 | M98 |
| 50705 | 1.4×10^{14} | 1.5×10^{10} | $\sim 420 / \sim 2000$ | FP98 |
| 51318 | 1.4×10^{14} | 1.5×10^{11} | ≤ 300 | FP00 |
| 51751 | 8.6×10^9 | 4.8×10^9 | ~ 600 | F01 |

PF97 = Pooley & Fender 1997; M98 = Mirabel et al. 1998; FP98, FP00 = Fender & Pooley 1998, 2000; F01 = this paper. The data from MJD 50583 (M98) were recorded simultaneously at *three* radio wavelengths.

tach meaningful error-bars to the resulting correlation function.

In order to remove the long term trend from the lightcurves, which could introduce spurious correlations into the correlation function, we subtracted a quadratic fit to the two data sets (‘detrending’) before calculating the DCF. The resulting DCF is shown in Figure 4; the strongest peak of the correlation function has a lag of 625 seconds, with a correlation coefficient of 0.47 ± 0.08 , although the feature is broad, which may indicate that a range of lags are present and/or reflect the less distinct pulse shape at the lower frequency (Fig 3). The DCF also shows secondary peaks at approximately ± 1800 seconds from the main peak, which are present in the auto-correlation function and are due to the periodic nature of the variability.

In Table 1 we summarise the frequency-dependent time

lags reported for the radio-infrared oscillations in GRS 1915+105. It is clearly of interest to know whether these times lags are variable. From table 1 it is clear that the data reported here are now the *second* case of different delays between the same two frequencies:

- (i) Pooley & Fender (1997) reported delays between 15 GHz and 8.3 GHz which were significantly shorter than those reported by Mirabel et al. (1998).
- (ii) The delay reported by Mirabel et al. (1998) between 5 – 8 GHz was also considerably longer than that reported between almost the same frequencies in this paper.

What could cause different time delays at different epochs? There are two obvious possibilities – different physical size scales at different epochs, or changes in the Doppler factor of the jet (since the delay between different frequencies originates in the relativistically flowing medium). In reality there may be some combination of these, and other, effects.

If the first explanation is the main reason however, we may expect some observational relation between radio flux levels and delays. The simultaneous 8 & 15 GHz light curves presented in Pooley & Fender (1997) had flux densities in the range 50–100 mJy. The oscillations presented in this paper have a range of about 40–100 mJy. The amplitudes reported in Mirabel et al. (1998), up to 100 mJy, appear to be somewhat larger. Thus the longer delays may be due to jet structure which is larger overall, and we would expect, given more data, to see a correlation between delay length and oscillation amplitude.

If the explanation is instead due to a changing Doppler factor, this may be most naturally explained as being due to a change in the angle of the jet to the line of sight (although we cannot rule out changes in the bulk Lorentz factor), for example if the jet is precessing. For a bulk Lorentz factor of 5 and angle of jet to the line of sight of ~ 65 degrees, as calculated for GRS 1915+105 ejections for a distance of 11 kpc (Fender et al. 1999), a swing of $\gtrsim 20$ degrees would be required in order to change the Doppler factor by the factor of ~ 2 indicated by table 1 (for larger Lorentz factors a smaller swing in angle is required, but this would have further implications for e.g. energetics). In the event that varying delays were caused by a periodically varying jet angle to the line of sight, we might expect to see, in the long-term, a repeating pattern of ‘long’ and ‘short’ delays.

5 CONCLUSIONS

In a set of high-sensitivity dual-frequency radio observations of GRS 1915+105 with ATCA during a period of radio oscillations we have captured in detail some key characteristics.

Firstly we have clearly shown that the GHz radio spectrum of GRS 1915+105 repeatedly cycles between optically thick and thin during periods of radio oscillations. While this could be qualitatively appreciated from previous sparse observations and simple concepts, we have for the first time captured the strong quasi-periodic signal in the radio spectrum. It can now be directly appreciated, from Fig 2, that were we to average over multiple oscillation events (for e.g. a weaker source or a shorter oscillation period), we would measure a spectral index which was a combination of both

optically thick and optically thin emission, with an average close to zero, as seen in hard states of black hole candidate X-ray binaries (Fender 2001). The transition from optically thin to flat/inverted radio spectra following the outburst is also reminiscent of the hard state transients (see e.g. Fig 3 of Fender 2001). In addition, the $\sim 1\%$ level of linear polarisation associated with the oscillations at both frequencies is comparable to that measured for the flat spectrum in the hard states of two black hole candidates, GS 2033+338/V404 Cyg (Han & Hjellming 1992), and GX 339-4 (Corbel et al. 2000), and this level of linear polarisation may be a generic feature of such flat spectra in BHC low/hard states (Fender 2001). The similarity of the linear polarisation position angle for both the optically thin flare and oscillations may indicate a preferred orientation of magnetic field for the outflow. In addition in this case we have measured the spectrum of the linear polarisation, and find it also to be approximately flat.

Finally, we have performed a cross-correlation analysis of the two radio lightcurves in order to establish a mean delay. This is the most thorough analysis of the time delays to date; previous attempts were ‘by eye’ or involved only the peaks of single events. Comparing all the reported frequency-dependent time delays for the oscillations from the literature, we find that there are significant differences at different epochs. The longest time delays reported seem to be associated with the large-amplitude oscillations in Mirabel et al. (1998), which may indicate a relation between event amplitude and subsequent time delay. However, at this stage a changing Doppler factor or some other effect cannot be ruled out.

Detailed observations such as these are crucial to a quantitative understanding of the physics involved in jet production, and may be vital in distinguishing between, for example, models of discrete ejections (e.g. van der Laan 1966; Mirabel et al. 1998) or shocks propagating along quasi-continuous flows (e.g. Blandford & Königl 1979; Kaiser, Sunyaev & Spruit 2000).

ACKNOWLEDGEMENTS

We would like to thank the referee, Ralph Spencer, for constructive criticism of this paper, and R. Ramachandran for a discussion about radio pulsar rotation measures. S.A.T. is thankful to RFBR for support (grant N98-02-17577). The Australia Telescope is funded by the Commonwealth of Australia for operation as a National Facility managed by CSIRO. RXTE ASM results were provided by the ASM/RXTE teams at MIT and at the RXTE SOF and GOF at NASA’s GSFC.

REFERENCES

- Belloni T., Mendez M., King A.R., van der Klis M., van Paradijs J., 1997a, ApJ, 479, L145
- Belloni T., Mendez M., King A.R., van der Klis M., van Paradijs J., 1997b, ApJ, 488, L109
- Belloni T., Klein-Wolt M., Mendez M., van der Klis M., van Paradijs J., 2000, A&A, 355, 271
- Blandford R., Königl A., 1979, ApJ, 232, 34

Chaty S., Rodriguez L.F., Mirabel I.F., Geballe T.R., Fuch Y., Claret A., Cesarsky C.J., Cesarsky D., 2001, *A&A*, 366, 1035

Corbel S., Fender R.P., Tzioumis A.K., McIntyre V., Nowak M., Durouchoux P., Sood R., 2000, *A&A*, 359, 251

Dhawan V., Mirabel I.F., Rodríguez L.F., 2000, *ApJ*, in press

Edelson R.A., Krolik J.H., 1988, *ApJ*, 333, 646

Eikenberry S.S., Matthews K., Morgan E.H., Remillard R.A., Nelson R.W., 1998, *ApJ*, 494, L61

Eikenberry S.S., Matthews K., Muno M., Blanco P.R., Morgan E.H., Remillard R.A., 2000, *ApJ*, 532, L33

Fender R.P., 2001, *MNRAS*, 322, 31

Fender R.P., Pooley G.G., 1998, *MNRAS*, 300, 573

Fender R.P., Pooley G.G., 2000, *MNRAS*, 318, L1

Fender R.P., Pooley G.G., Brocksopp C., Newell S.J., 1997, *MNRAS*, 290, L65

Fender R.P., Garrington S.T., McKay D.J., Muxlow T.W.B., Pooley G.G., Spencer R.E., Stirling A.M., Waltman E.B., 1999, *MNRAS*, 304, 865

Feroci M., Matt G., Pooley G., Costa E., Tavani M., Belloni T., 1999, *A&A*, 351, 985

Foster R. S., Waltman E. B., Tavani M., Harmon B. A., Zhang S. N., Paciesas W. S., and Ghigo F. D. 1996, *ApJ*, 467, L81

Gaskell C.M., Peterson B.M., 1987, *ApJS*, 65, 1

Giovannini G. et al., 2001, *Ap&SS*, 276, 111

Han X., Hjellming R.M., 1992, *ApJ*, 400, 304

Han J.L., Manchester R.N., Qiao G.J., 1999, *MNRAS*, 306, 371

Kaiser C.R., Sunyaev R., Spruit H.C., 2000, *A&A*, 356, 975

Klein-Wolt M., Fender R.P., Pooley G.G., Belloni T., Migliari S., Morgan E.H., van der Klis M., 2001, *MNRAS*, submitted

Levine A.M., Bradt H., Cui W., Jernigan J.G., Morgan E.H., Remillard R.A., Shirey R., Smith D., 1996, *ApJ*, 469, L33

Merloni A., Fabian A.C., Ross R.R., 2000, *MNRAS*, 313, 193

Mirabel I.F., Rodríguez L.F., 1994, *Nature*, 371, 46

Mirabel I.F., Dhawan V., Chaty S., Rodríguez L.F., Martí J., Robinson C.R., Swank J., Geballe T.R., 1998, *A&A*, 330, L9

Morgan E.H., Remillard R.A., Greiner J., 1997, *ApJ*, 482, L155

Naik S., Rao A.R., 2000, *A&A*, 362, 691

Pooley G.G., Fender R.P., 1997, *MNRAS*, 292, 925 [PF97]

Rodríguez L.F., Gerard E., Mirabel I.F., Gomez Y., & Velazquez A., 1995, *ApJ Supp.*, 101, 173,

Rodríguez L.F., Mirabel I.F., 1999, *ApJ*, 511, 398

Trushkin, S., Majorova, E., Bursov, N., 2001, *Ap&SS*, 276, 135

van der Laan, H., 1966, *Nature*, 211, 1131